Author(s): Miettunen, Kati & Asghar, Imran & Mastroianni, Simone & Halme, Janne & Barnes, Piers R.F. & Rikkinen, Emma & O Regan, Brian C. & Lund, Peter

Title: Effect of molecular filtering and electrolyte composition on the spatial variation in performance of dye solar cells

Year: 2012

Version: Post print

Please cite the original version:

Miettunen, Kati & Asghar, Imran & Mastroianni, Simone & Halme, Janne & Barnes, Piers R.F. & Rikkinen, Emma & O Regan, Brian C. & Lund, Peter. 2012. Effect of molecular filtering and electrolyte composition on the spatial variation in performance of dye solar cells. Journal of Electroanalytical Chemistry. Volume 664. 63-72. ISSN 1572-6657 (printed). DOI: 10.1016/j.jelechem.2011.10.012.

Effect of molecular filtering and electrolyte composition on the spatial variation in performance of dye solar cells

Kati Miettunen[*,a,b], *Imran Asghar*[a], *Simone Mastroianni*[c], *Janne Halme*[a], *Piers R. F. Barnes*[b], *Emma Rikkinen*[d], *Brian C. O'Regan*[b],*and Peter Lund*[a]

[a)] Department of Applied Physics, Aalto University, P.O. BOX 15100, FIN-00076 Aalto, Finland

[b)] Department of Chemistry, Imperial College London, London SW7 2AZ, UK

[c)] Department of Electronics Engineering, University of Rome "Tor Vergata", CHOSE Lab, Via Giacomo Peroni 400/402, 00131 Rome, Italy

[a)] Department of Biotechnology and Chemical Technology, Aalto University, P.O. BOX 16100, FIN-00076 Aalto, Finland

* Corresponding author: Telephone: +358 9 451 8253.

E-mail address: kati.miettunen@tkk.fi

Abstract

It is demonstrated that the molecular filtering effect of TiO_2 has a significant influence on dye solar cell (DSC) performance. As electrolyte is injected to a DSC, some of the electrolyte components adsorb to the surface TiO_2 (here 4-*tert*-butylpyridine and 1-methyl-benzimidazole) and accumulate near the electrolyte filling hole resulting in varying electrolyte composition and performance across the cell. The spatial performance distribution was investigated with a new method, the segment cell method. Not only is the segmented cell method simple and cheap when compared to the only other method for examining spatial variation (photocurrent mapping), it also has the major advantage of allowing the spatial variation in all other operating parameters to be assessed. Here the molecular filtering effect was to influence the cell performance in case of all the five studied electrolytes causing up to 35 % losses in efficiency. Raman spectra indicated that the loss in photocurrent in the electrolyte filling was in correlation with the loss of thiocyanate ligands suggesting that dye regeneration may also be a significant factor in addition to electron injection in some of the cells. There were also shifts in the absorption spectra the photoelectrodes which further supported changes in the thiocyanate ligands. Besides absorption changes, there were additional shifts in the IPCE spectra which may relate to deprotonation of the dye. The efficiency losses were reduced to ~10 % with contemporary electrolyte compositions.

Keywords: Dye-sensitized; Up-scaling; Spatial distribution; Electrolyte filling; Thiocyanate ligand.

1. Introduction

Dye solar cells (DSC) are an attractive alternative to conventional *pn*-junction solar cells due to their cheap materials and easy manufacturing methods which can even be transferred to roll-to-roll mass production. Over 10 % efficiencies have been demonstrated in small scale [1] and the transferring of the DSC technology to large scale has begun. The efficiencies are lower in large scale [1,2] as in part due to resistive losses from current collection as the cell size increases. In some studies, the differences in the performance of small cells (2.5 cm^2 active area) and modules (900 cm^2 active area) have actually been relatively small.[2-4] However this appears not be generally the case, for example our earlier results showed that significant efficiency losses (~20 %) occur due to the electrolyte filling when the cell size is increased from 0.4 cm^2 to only 1.2 cm^2,[5] the smaller area is typical of the size tested for record efficiency cells. The changes were independent of resistive losses.

That initial study indicated that 4-*tert*-butylpyridine (4-tBP), a common additive in DSC electrolytes, adsorbs to the TiO_2 unevenly so that the area near the electrolyte filling hole had the highest concentration which decreases in the regions further away from the hole.[5] Moreover, it was noted that these differences did not decrease over time but rather increased.[5] The spatial variation of cell performance that results from electrolyte filling represents a major challenge for the commercialization of DSCs. Even relatively minor reductions in the efficiency of manufactured modules can have a very significant impact on the economic viability of the technology. To avoid these performance losses, either the electrolyte composition or its application method need to be developed.

In this contribution we focus on modification of the electrolyte composition to avoid, or at least reduce, the spatial losses caused by the conventional electrolyte filling method without compromising the cell efficiency. The main task is to investigate which of the commonly used electrolyte components have tendency to cause spatial performance variation. We use the segmented cell method that was introduced briefly in our previous study shown in the context of the initial results.[5] The dimensions of the segmented cells used in this study are roughly similar to a single stripe of a DSC mini module such as the ones used in our previous study.[6] In addition to detecting the spatial variation in the photovoltaic performance with segmentation, Raman and incident-photon-to-current-efficiency (IPCE) measurements are executed to further investigate the underlying causes of the performance variation.

2. Experimental methods

2.1. Cell preparation

The different electrolyte compositions are given in Table 1. The chemicals used for the preparation of the electrolytes were: iodine (I_2, Sigma-Aldrich, ≥ 99.8 %), 4-*tert*-butylpyridine (4-tBP, Aldrich, 96 %), 1-Methyl-benzimidazole (NMBI, Aldrich, 99%), Lithium iodide (LiI, Aldrich, 99.9 %), 1-propyl-3-methylimidazolium iodide (PMII, Solaronix), Guanidinium thiocyanate (GuSCN, Sigma, ≥ 99 %), 3-methoxypropionitrile (MPN, AlfaAesar, 99 %). A commercial electrolyte high stability electrolyte (HSE) by DyeSol was also tested.

Table 1. Electrolyte composition given as molar concentrations

Electrolyte name	I_2	TBP	NMBI	LiI	PMII	GuSCN	Solvent
TBP-LiI	0.05	0.5		0.5			MPN
NMBI-LiI	0.05		0.5	0.5			MPN
NMBI-PMII	0.05		0.5		0.5		MPN
NMBI-PMII-GuSCN	0.05		0.5		0.5	0.1	MPN

The photoelectrodes consisted of a screen printed thermally treated TiO_2 film (DyeSol 18NR-T, two layers with total thickness ~7 µm) deposited on fluorine-doped tin oxide (FTO) coated glass substrates that were sintered at 450 °C for 30 min. After that the films were sensitized in a dye bath using a dye solution consisting of 0.32 mM *cis*-bis(isothiocyanato)bis(2,2'-bipyridyl-4,4'-dicarboxylato)-ruthenium(II) bis-tetrabutylammonium (DyeSol) in ethanol (99.5 wt-%). The counter electrodes were thermally platinized FTO glass substrates. Detailed specifications of the electrode preparation are given elsewhere.[5] The electrodes were sealed with a 25 µm thick Surlyn ionomer resin film spacer (DuPont) and the electrolyte was injected to the cell through filling channels drilled in the counter electrode substrate. The filling holes were sealed with a Surlyn foil and a thin cover glass.

2.2. Segmented cells

a)

Figure 1. a) Schematics and b) a photo of a four segment cell. The segments are electrically isolated (marked by dashed lines in the schematics) but share the same electrolyte layer.

In the analysis we used 4-segment cells in which the conductive FTO layer of the substrates was divided into electrically isolated segments with laser scribing (Figure 1). The 4-segment cells are compared with simultaneously prepared small single cells having the same geometry and size of the dyed TiO_2 layer as in an individual segment. The segments are numbered from 1 to 4, the one nearest to the electrolyte filling hole is marked as segment 1 as indicted in Figure 1a. The segmented cells were prepared with sufficient randomization to avoid systematic errors in the examination of the main effect, here the electrolyte filling direction. In this work special care was taken in this regard: for instance the electrolyte was filled from different ends of the different cells so that neither the application of the TiO_2 film nor the position in the oven during the heat treatments can

have any effect even though their effect is expected to be negligible. Furthermore, it was tested that the measurement order of the segmented cell does not affect the results.

The basic idea of the method is to section the electrodes of the cell to electrically isolated areas that share the same electrolyte layer, and from each of them all the photovoltaic parameters can be measured independently. This is a major advantage compared to previous techniques; for instance with photocurrent imaging only spatial variations in the short circuit current can be observed.[7,8] There are, however, some limitations that need to be taken into account: If the electrical cuttings on the photoelectrode and counter electrode are not aligned accurately enough, ions in the electrolyte can move between the different segments when current is drawn from the cell and it can cause drifts in the data. We calculated using a 2D dye solar cell model [10] that the maximum tolerance for the misalignment is in the range of 10 µm. In practice this means that it is not practically possible to get the electrodes aligned that well and there will be drifts. The drifts are, however, relatively slow; it takes almost ten minutes for the ions to diffuse over the distance of 0.5 mm between the adjacent segments [9] and here the distance between the segments was even larger (2 mm). This means that short measurements (in the range of a couple of minutes) such as IV and IPCE are not significantly affected whereas hours long electrochemical impedance spectroscopy (EIS) measurements very likely are. The drift of ions, as it affects also tri-iodide, will cause a clear change in the electrolyte color meaning that besides modeling, their effect can be also visually monitored. With proper selection and monitoring of the measurements, the segmented cell method is very efficient in the

study of spatial variation in particular when the changes between the segments are very large as in this study.

2.3. Measurements

The photovoltaic performance was measured using a solar simulator providing 1000 W/m^2 AM1.5G equivalent light intensity.

IPCE measurements and transmission spectra were taken using Model QEX7 Solar Cell Spectral Response Measurement System from (PV Measurements, Inc.) in DC mode without bias illumination. IPCE Spectra were measured in the range of 300-800nm with intervals of 20 nm from both counter-electrode (CE) and photo-electrode (PE) side at the short circuit conditions. A silicon photodiode was used for calibrating the system in the 300-1000 nm wavelength range.

The Raman spectra of the DSCs were measured using a HORIBA Jobin Yvon LabRam 300 micro-Raman spectrometer equipped with a 514 nm argon laser. The power of the argon laser was 1.24 mW which was reduced to 1% using a filter in the measurements. The spot size was approximately 5000 µm^2 leading to laser light intensity of about 2500 W/m^2. Here we used the same laser source with same incident power, using the same detecting system, the same 5 s time for a single measurement, and following all the measurement procedures in a similar fashion for all the samples in order to maximize the comparability of the data. The FTO glass in the actual segmented cells was too thick to get enough scattered Raman signals. Therefore in the samples that were used in the Raman

measurements, the counter electrodes were replaced with 1 mm thick microscope glasses and the measurements were carried out through that side.

3. Results and discussion

3.1. Photovoltaic performance

Five different electrolyte compositions which are representative of those normally used in the field were examined. The electrolyte 4-tBP-LiI is a conventional type of electrolyte that has been the basis for different variations since 1990s and has been used in larger DSCs as well.[3,10] Both 4-tBP and LiI have been questioned due to stability issues, the former mainly because of purity of the currently commercially available materials and the latter due to inherent effects. Regardless of this they are still commonly used in the field, in particular to reach high efficiencies. Table 2 shows that with 4-tBP-LiI electrolyte there were large performance variations between the different segments: Going from segment 1 to 4, the short-circuit current density (J_{SC}) increases gradually as much as 240 % while both the open-circuit voltage (V_{OC}) and the fill factor (*FF*) decreases gradually by 20 %. All in all, the efficiency (η) of individual segments varied from 1.7 % to 4.1 %. The calculated electrical parallel connection of the four segments represent an estimation of the overall performance of the corresponding stripe-like cell in a small DSC module. In this case the parallel connection had an efficiency (η) of 3.0 % i.e. only ~65 % of that of a small individual reference cell. In practice this means that if 4-tBP-LiI electrolyte was used in a DSC module filled with the electrolyte this way, the efficiency losses caused by uneven spatial performance variation would likely be the largest loss mechanism related to the up-scaling.

Replacing 4-tBP with NMBI, a commonly used alternative additive that also boosts V_{OC}, did not change the results much (Table 2). The only practical difference was the somewhat larger variation in *FF* with NMBI-LiI electrolyte than with 4-tBP. A few hours after the cell assembly, there were also visual differences between the segments in the NMBI-LiI cells: there was gradual loss of electrolyte color when going from segment 1 to 4 and increase of dark clusters, which were presumed to be co-crystals of NMBI and iodine. A corresponding color change could be seen also in the small NMBI-LiI reference cells as well, however, in smaller scale. The crystallization reaction between NMBI and iodine has been reported in the literature in detail.[11] Here, the hypothesis for this reaction is that there is initially the same amount of dissolved iodine in all the segments as it is compatible with visual observations. The other electrolyte components such as NMBI distribute unevenly which apparently changes the solubility of tri-iodide resulting in crystallization of iodine in the segments farther from the filling hole. Thus there is bleaching of the electrolyte around the dark spots of crystalline I_2. In the cells with other electrolytes, there were no such visual changes. This is likely related to the fact that the other electrolyte components such as GuSCN affect the crystallization reaction.[11]

Like 4-tBP, LiI is also a conventional electrolyte component. The purpose of LiI is to be a source of I^- ions and to shift the conduction band of TiO_2 down which helps in the electron injection increasing the photocurrent. Leaving LiI out of the electrolyte and having PMII instead as a source of I^- ions, the J_{SC} of the small reference cells was lower, as to be expected (Table 2). However with the NMBI-PMII electrolyte, the performance of

individual segments, namely J_{SC} was significantly more even (~5 % variation) compared those cells than contained LiI (240 % variation) (Table 2). Interestingly the middle segments (2 and 3) have also ~5 % higher J_{SC} compared to outer segments (1 and 4). Only a small 5% gradual decrease of V_{OC} from segment 1 to 4 was observed which suggests that there was an uneven distribution of NMBI. The overall result was that the performance of parallel connected segments with NMBI-PMII electrolyte was actually very close to that of small reference cell (Table 2).

In recent years, it has become very common to add GuSCN to the electrolyte instead of LiI to boost the photocurrent and hence also the efficiency. Indeed with NMBI-PMII-GuSCN the efficiency of the small reference cell was higher than with all the other electrolytes. The same applies to the parallel connected segmented cells, even though having GuSCN in the electrolyte actually increased the variation in the performance of the segments compared to NMBI-PMII; there was e.g. 10 % decrease of V_{OC} from segment 1 to 4 (Table 2). Interestingly, the behavior of a commercially available electrolyte of an unknown composition, HSE from Dyesol, was quite similar to the NMBI-PMII-GuSCN electrolyte, suggesting a similar composition. Indeed, the Raman spectroscopy results discussed later in the paper point to the presence of GuSCN in the HSE electrolyte.

The systematic decrease of V_{OC} from segment 1 to 4 is seen with all the studied electrolytes. In our initial study with 4-tBP-LiI electrolyte similar effect was seen and it was related to electrolyte filling as that is the only practical difference between the segments and furthermore the performance of the segments could be modified by changes in the

electrolyte filling.[5] This response can be understood as follows: as the electrolyte along the surface of TiO_2 layer, quickly adsorbing components of the electrolyte attain higher concentration near the electrolyte filling hole (i.e. the nanoporous TiO_2 film behaves as a filter). It is well known that 4-tBP and NMBI increase V_{OC} and therefore the decreasing of V_{OC} suggests a drop in their concentration. The molecular filtering effect suggested here is conceptually similar to the phenomenon used in chromatography. The significance of the effect on DSC performance is striking and it has been completely ignored in the past apart from our initial results.[5]

The molecular filtering effect could theoretically be affected by the speed of electrolyte filling (rate of adsorption vs. speed of the electrolyte flux in the filling). Indeed, this common filling technique used here is most likely one of the slowest ones to fill the cell and the filtering effect might be expected to be enhanced relative to other quicker electrolyte filling methods. It was, however, confirmed using an electrolyte similar to the NMBI-PMII-GuSCN electrolyte and fast vacuum pump assisted filling that the spatial variations did not reduce. This suggests that the rate of electrolyte species adsorption is much quicker than the filling speed of typical electrolyte insertion methods.

Although the spatial performance variation was significantly evened out by using modern electrolyte compositions (NMBI-PMII and NMBI-PMII-GuSCN) instead of the traditional ones, it could not completely be omitted. For instance, with NMBI-PMII-GuSCN electrolyte the efficiency of the parallel connected cell was still 10 % lower efficiency compared to the small reference cell, which is significant from industrial perspective. From

a practical point of view one of the most problematic issues is that liquid electrolytes which have been shown to give good stability and performance include a voltage increasing agent, either tBP or NMBI (or similar e.g. BI). As shown here, both 4-tBP and NMBI appear to be causing problems and thus finding a commercially interesting electrolyte composition which would not be subject to this effect remains an important challenge.

The spatial performance variation of J_{SC} was the largest in the cells with presence of LiI (and absence of PMII) in the electrolyte. Interestingly enough, in our previous study, the performance of electrolyte containing merely LiI and I_2 in the electrolyte solution resulted in quite uniform performance in the 4-segment cells.[5] Hence, it appears that LiI alone would not cause spatial variation problems. Here it was used only with either 4-tBP or NMBI, which indicates that there may be chemical interactions between Li^+ and these additives. It has been reported that 4-tBP forms complexes with Li^+ which then reduces the interaction of Li^+ ions with the TiO_2 film.[12,13] Hence in the segments with elevated local concentrations of 4-tBP and NMBI there could then be a reduction of the amount of Li^+ ions. This would then lead to an even higher shift of the TiO_2 conduction band which would in turn reduce electron injection efficiency. In later sections we address whether changes electron injection are the only factor affecting J_{SC}.

Table 2. Typical performance characteristics of the individual segments and their parallel connection in comparison to the small reference cell when using different electrolytes.

	J_{SC} (mA/cm^2)	V_{OC} (mV)	*FF* (%)	η (%)
4-tBP-LiI				
segment 1	3.1	759	72	1.7
segment 2	7.0	779	61	3.3
segment 3	9.9	717	58	4.1
segment 4	10.2	616	57	3.6
parallel connection	7.5	698	57	3.0
small reference	9.9	731	62	4.5
NMBI-LiI				
segment 1	4.6	752	70	2.5
segment 2	8.3	762	60	3.8
segment 3	9.4	732	55	3.8
segment 4	10.4	624	43	2.8
parallel connection	8.2	714	51	3.0
small reference	9.7	757	61	4.5
NMBI-PMII				
segment 1	8.7	758	66	4.3
segment 2	9.3	728	65	4.4
segment 3	9.6	717	64	4.4
segment 4	8.8	717	65	4.2
parallel connection	9.1	729	65	4.3
small reference	8.7	754	67	4.4
NMBI-PMII-GuSCN				
segment 1	9.2	797	66	4.8
segment 2	10.0	746	65	4.9
segment 3	10.2	721	65	4.8
segment 4	9.3	705	64	4.2
parallel connection	9.7	739	65	4.6
small reference	10.1	768	67	5.2
HSE				
segment 1	9.9	743	62	4.5
segment 2	10.6	676	64	4.6
segment 3	10.7	639	62	4.3
segment 4	10.1	642	63	4.1
parallel connection	10.3	667	63	4.3
small reference	10.9	704	66	5.1

3.2. Raman spectroscopy

As the photovoltaic data suggests variations in the 4-tBP and NMBI concentration across the segmented cells, we wanted to examine those with Raman. The intensity of a Raman peak $I(v)$ is given by [14]

$$I(v) = I_0 K(v) C \quad (1)$$

where I_0 is the intensity of the incident laser light, $K(v)$ includes the frequency dependent terms, v is the Raman shift in cm^{-1}, and C is the concentration of corresponding specie. Assuming that the intensity of the laser power and frequency dependent factors remain constant, the intensity of species peak at a particular Raman shift is directly proportional to its concentration. The height of the Raman peak has been therefore been used to estimate the concentration of different species.[14]

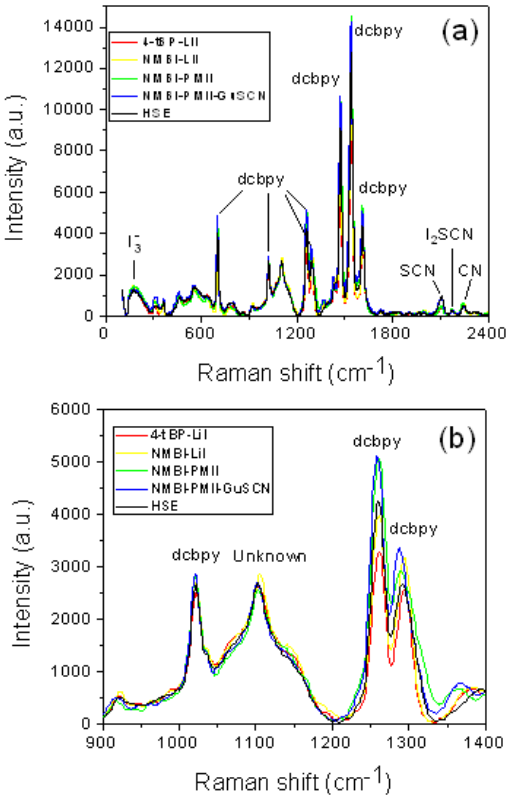

Figure 2. Comparison of Raman spectra at the photoelectrodes of reference cells with the different electrolytes at range a) 0-2400 cm^{-1} and b) 900-1400 cm^{-1}.

The Figure 2 shows the Raman spectra of the reference cells with the different electrolytes. The analysis of the Raman spectra reveals that the changes between the electrolytes cause differences only in the intensity of some of the peaks, but otherwise the form of the spectra is rather similar. Based on the literature of the Raman peak for 4-tBP should appear at 996 cm^{-1} and that for NMBI around 1360 cm^{-1}.[15,16] However, Figure 2b does not show any peaks in those regions which apparently means that the 4-tBP and NMBI have very weak Raman signals. The samples in the literature were, however, only based on mixture of MBI and LiI in MPN or 4-tBP liquid whereas here the Raman spectroscopy was done on

complete DSCs which also includes dyed TiO_2 films. Other studies of complete DSC do not mention these peaks either.[16,17]

As Figure 3 indicates, there were instead significant differences in spectra around 2106 cm^{-1} which has been associated with the characteristic peak of thiocyanate (SCN^-) ligand.[17] The SCN^- ligand attached to the Ru atom of the dye is involved in regenerating the dye. The 4-tBP-LiI and NMBI-LiI show a significant increasing trend both in the intensity of the SCN^- from segment 1 to segment 4 (Figures 3a and b) and in the short circuit current (Table 2). Figure 3f shows clearly that with SCN^- peak height below ~500 a.u., there is a strong correlation between J_{SC} and the amount of SCN^- measured using Raman. Therefore it is plausible to assume that the low J_{SC} in some of the cells may be limited by the regeneration of the dye due to smaller SCN^- concentration. Above peak height 500 a.u., J_{SC} is not apparently limited by the amount of SCN^- in the cell and the increase in SCN^- does not improve J_{SC} any further (Figure 3f). The J_{SC} data in Figure 3f can be fit by a simple phenomenological model (see figure caption) in which the SCN^- peak intensity assumed to be proportional to the rate of charge separation in the dye molecules (due regeneration and/or electron injection) where this process competes with an approximately constant rate of electron-dye recombination or excited state decay. Since our data suggests that it is likely that regeneration in addition injection efficiency is influenced by the spatial variation of electrolyte additives, the mechanism influencing photocurrent is almost certainly more complex than the simple model presented in the figure caption and we do not pursue this further here. More detailed measurements of regeneration would be required to reach a quantitative understanding.[18]

Associating the peak at 2106 cm^{-1} with the amount of SCN^- attached to the dye is further confirmed by significantly higher peak in the NMBI-PMII-GuSCN cells (Figure 3) where additional SCN^- is present at high concentrations in the electrolyte due to GuSCN. The peak is similarly high with the HSE electrolyte pointing to the presence of GuSCN or other source of SCN^- in the electrolyte. In case of these cells, the J_{SC} values were higher and did not vary as much as those without GuSCN (Table 2). As mentioned before, this could be interpreted as the cells with GuSCN not being limited by regeneration of the dye. It appears that the variation in the intensity of the SCN^- representing the concentration of the SCN^- is indeed related to differences in J_{SC}.

Substitution of SCN^- with 4-tBP and NMBI has been reported in the literature and furthermore it has been stated that differences in the electrolyte composition trigger these substitution processes.[16-18] Any degradation of the dye due to the SCN^- ligand substitution could decrease J_{SC} of the DSC if J_{SC} is limited by the regeneration of the dye. Above all, the SCN^- peak is lower for segments with low J_{SC} and high V_{OC} in which regions according the deductions based on photovoltaic performance NMBI or 4-TBP are in larger quantities. Here SCN^- exchanges most probably with NMBI and/or 4-TBP. On the basis of the photovoltaic performance it seem possible that the there are also fewer Li^+ are on the TiO_2 surface where there is more NMBI or 4-tBP. Interestingly, it has been reported that presence of Li^+ ions indeed protects SCN^- ligand from the exchange by MBI by forming a complex between Li^+ and MBI and therefore their amounts should be carefully optimized.[16] It seems likely that Li^+ prevents ligand exchange also in the case of NMBI and 4-tBP.

Hence it appears logical that the segments with high concentration of NMBI or 4-tBP with few Li^+ there would be loss of SCN^- ligands due to exchange reactions. When large PMI^+ ions was used instead of small Li^+, there are no such large differences in the peak heights as indicated by Figures 3b and c which suggests that the PMI^+ protects SCN^- ligand from exchange reactions. Indeed, it has been stated also in the literature that bulky counter ions protect SCN^- ligand better compared to small Li^+ ions.[16]

One issue with the Raman measurements is that the very high local light intensity in the Raman beam could potentially cause artifacts in the data by temporarily or permanently changing the dye or its ligands. In some studies the high intensity Raman beam has been indeed used to purposely degrade the cells, but there the intensity of the laser was 6 orders of magnitudes higher.[17] Here the aim was reduce/avoid such effects by finding an optimum: reducing the beam intensity and measurement time but keeping them sufficiently high to get good quality data. Here at least no defects or artifacts were seen after the measurements which are a clear signs of such stability problems. This does not rule out the possibility of lesser changes in the sample. As the light intensity of the laser is still high compared to e.g. conditions in a solar simulator, it may affect the time for which a dye stays in oxidation state. Although the SCN peak in the Raman spectra could be induced by the laser partly or even solely, even in that case the Raman spectra would still give information about the spatial distributions in the electrolyte. The interpretation in that case would be that the electrolyte composition in the different parts of the cell would have varying ability to regenerate the dye, which is basically the same main conclusion that was presented for the

case in which the beam was not expected to affect the Raman spectra. Thus, in any case the effect of spatial distribution of electrolyte is clear.

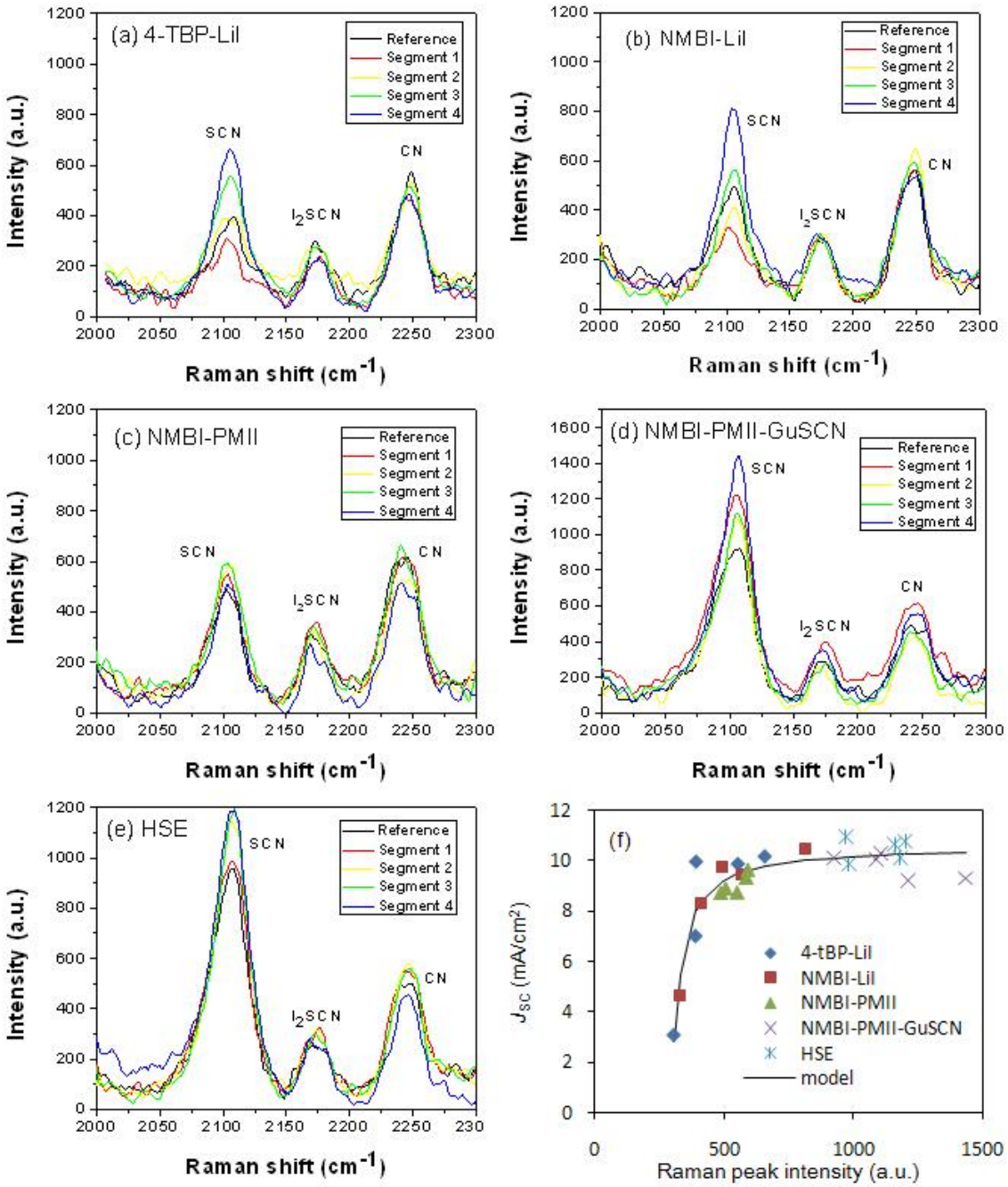

Figure 3. Comparison of Raman spectra (2000 – 2300 cm^{-1}) at the photoelectrodes of segmented cells and corresponding reference cell using electrolyte a) 4-tBP-LiI, b) NMBI-LiI, c) NMBI-PMII, d) NMBI-PMII-GuSCN and e) HSE. f) The SCN^- peak heights of all the segmented and reference cells vs. J_{SC}. The solid line is a phenomenological model fitted to the data: $J_{SC} = J_{MAX}\ (I-I_0)/[(I-I_0)-R]$ where J_{MAX} is maximum photocurrent expected from the device I_0 is a background SCN^- peak intensity and R is a recombination (or decay) term inhibiting regeneration (or injection). The fit parameters are $J_{MAX} = 10.5\ mA/cm^2$, $I_0 = 294$ and $R = 30.7$.

3.3. Optical changes

The spatial variation in the electrolyte additives influences the optical absorption of the films. Figure 4 shows an example of transmission (T) measurements where normalized spectra of 1-T for the series of segments with electrolyte containing Li^+ and 4-tBP were plotted. The spectra of the segments are increasingly red shifted as the electrolyte has passed through/across an increasing quantity of nanoparticulate TiO_2.

The changes in 1-T spectra relate to changes absorption. These changes are consistent with the differences observed in the Raman spectra (Section 3.2) and shed light on the role of thiocyanate ligand. As is well known in literature, SCN^- ligands are used for tuning the spectral response of a dye towards the red.[19,20] Thus SCN^- exchanged from the dye molecules with 4-tBP in electrolyte, corresponding to a reduction in the SCN^- peak at around 2106 cm^{-1}, would also correspond to a blue shift in the cell absorption spectrum as observed.

In order to give an estimation of this phenomenon one can consider that the substitution of one of the two SCN^- in the N719 dye with 4-tBP gives about 30 nm IPCE shift towards blue side.[21] The comparison of optical and IPCE spectra show 15 nm blue shift in the transmittance (Figure 4) and an almost 20 nm IPCE blue shift from segment 4 to segment 1 (Figure 5). This gives a rough estimation that ~25% of SCN^- ligands are exchanged in the first segment.

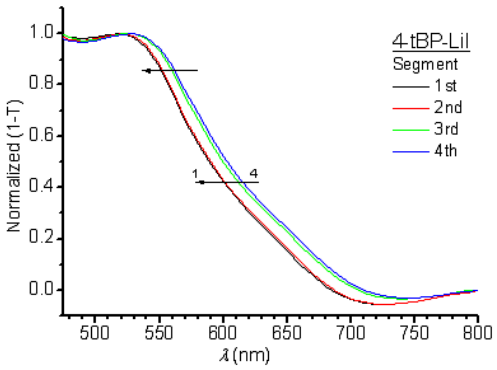

Figure 4. Comparison between the normalized (1-T) for segment 1 to 4 for segmented cell with electrolyte 4-tBP-LiI. The arrows show the blue shift from segment 4 to 1.

3.4. IPCE analysis

Incident-photon-to-collected-electron (IPCE) measurements were carried out to study the partial quantum efficiencies of the photocurrent generating processes of the cell. The total IPCE efficiency (η_{IPCE}) for a given wavelength (λ) is composed of four different factors which are the light harvesting (η_{LH}), the electron injection (η_{INJ}), the charge collection (η_{COL}) and the regeneration efficiencies (h_{REG}):[22]

$$\eta_{\mathrm{IPCE}}(\lambda) = \frac{J_{\mathrm{SC}}(\lambda)}{q\phi(\lambda)} = \eta_{\mathrm{LH}}(\lambda)\eta_{\mathrm{INJ}}(\lambda)\eta_{\mathrm{COL}}(\lambda)\eta_{\mathrm{REG}}(\lambda) \qquad (2)$$

where $J_{SC}(\lambda)$ is the short circuit current density, q is the elementary charge and $\varphi(\lambda)$ is the photon flux. The IPCE spectra were measured from both photo-electrode (PE) and counter-electrode (CE) side. The different additives in the electrolyte are responsible for particular features of the IPCE spectra and therefore changes in their quantity can be evaluated from that basis.

If variations in the IPCE due to differences in light harvesting and electron collection losses can be neglected, the quantum efficiency (QE) peak height should be approximately proportional to J_{SC}. Figure 5f shows that relationship between J_{SC} and QE maximum is roughly linear with the exception of a few single points.

The reasons for the large differences on η_{IPCE} peak height relate to changes in η_{LH}, η_{INJ}, η_{COL} and/or η_{REG}. The Raman spectra indicated strongly that there may be differences in η_{REG}. However, it cannot be quantitatively determined if η_{REG} is the only or even a dominating factor. By process of elimination, we can deduce which of the other factors can be causing the major differences in the peak value of the IPCE spectra.

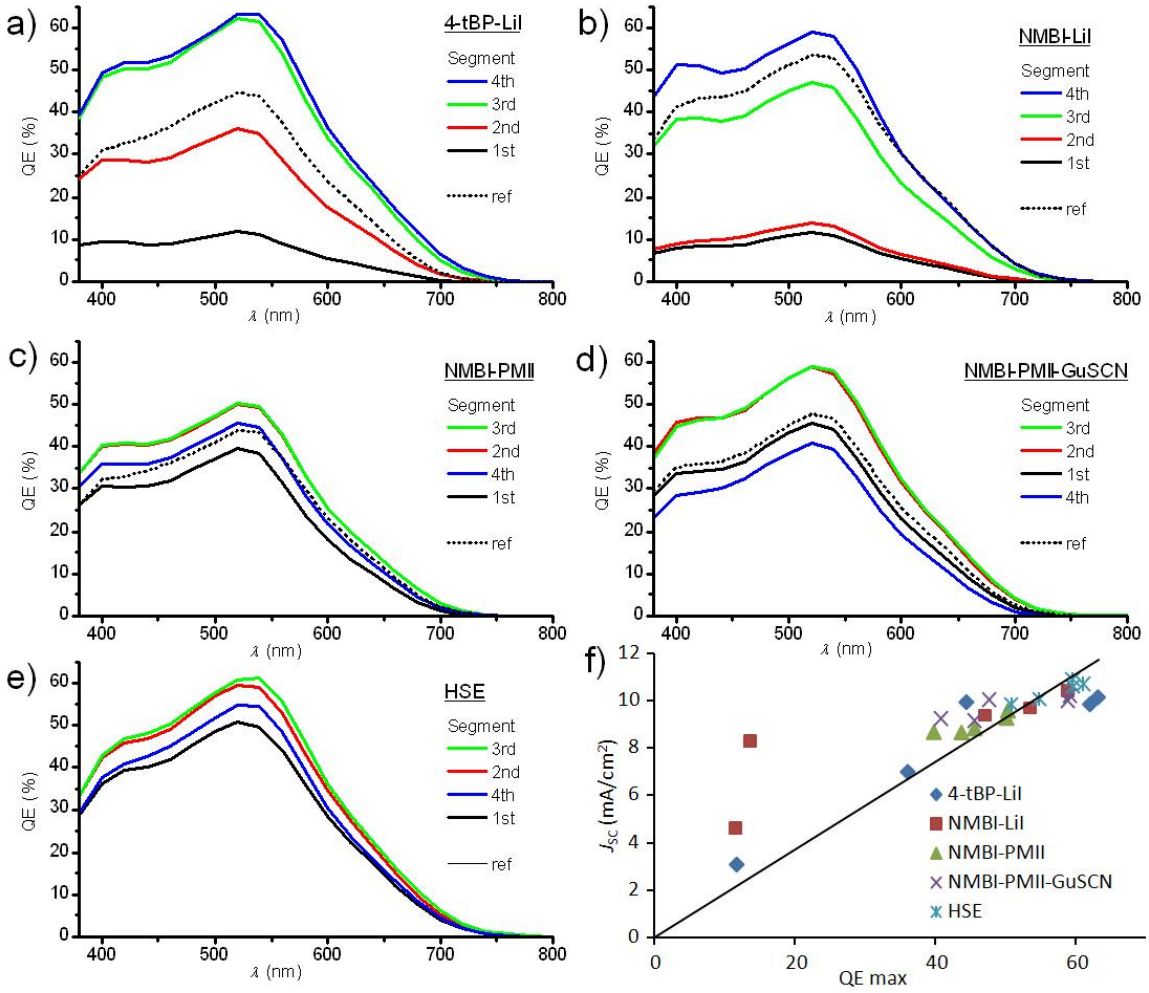

Figure 5. a-e) η_{IPCE} from the PE side of the cells with the different electrolytes. Each graph shows the values for the 4 different segments of the same cell from black curve (first segment) to blue curve (forth segment) and the value of the reference small non-segmented cell is given by dashed black curve. Plot f) represents the quantum efficiency peak value for the different segments (at about 530 nm) of cells vs. the J_{SC} values. Figure f shows also a linear trend line fitted to all the points and it is set to go via origin. The legends are organized in the order of decreasing IPCE peak in Figures a-e.

Firstly, the cells were optically quite similar; there were some differences in the absorption as mentioned in the previous section and for cell with NMBI-LiI electrolyte there were also visible differences in the electrolyte of different segments and cells with electrolyte HSE have deeper yellow color compared to the others. These differences cause some shifts in the spectral shape, but cannot explain the large difference in the peak heights and hence η_{LH} cannot be the dominating factor causing the difference in the J_{SC}.

Secondly, the comparison of IPCE data from PE and CE side (data not shown) reveals that the primary difference between the PE and CE illumination can be accounted for by differences in electrolyte absorption, thus η_{COL} cannot explain the major differences in J_{SC} either.

Hence, it appears also on the basis of IPCE measurements that the dominant differences in J_{SC} values are likely to be caused by either η_{INJ} or η_{REG}. Regarding difference in η_{INJ}: As well documented in the literature the shift of the TiO_2 conduction band occurs toward more negative potentials for 4-tBP or NMBI and toward more positive potentials for Li^+.[23-28] As the conduction band shifts, it makes the overlap between the TiO_2 acceptor states and the singlet and triplet dye excited states to decrease (with 4-tBP and NMBI) or increase (with Li^+).[29-33] Hence, the addition of Li^+ facilitates fast electron injection while 4-tBP adsorption leads to fewer injected electrons.[33] The apparent differences in 4-tBP or NMBI and possibly also with Li^+ quantities across the different segments in the case of 4-tBP-LiI and

NMBI-LiI electrolytes could cause the low in η_{INJ} near the electrolyte filling hole leading to decreased J_{SC} in that area.

Regeneration rate, besides I^- concentration,[34] is ruled by the thickness of the Helmholtz double layer which is dependent on the adsorbed cations [30] and on ability of cations to penetrate between the adsorbed dye and the TiO_2.[24] A thinner double layer causes I^- to efficiently adsorb onto the oxide.[35,36] The small cation Li^+ is able to intercalate into the TiO_2 thus reducing the Helmholtz layer, while in the presence of 4-tBP or NMBI its adsorption is suppressed.[25] This last phenomenon causes anions to experience in relative terms less Coulombic attraction to penetrate between the dye and TiO_2, thus reducing the regeneration rate of the oxidized dye by I^-. This could contribute to a reduction in the η_{IPCE} peak and, hence, result in a lower J_{SC}.[37] This could also explain why in the Li^+ containing cells (4-tBP-LiI and NMBI-LiI) there is low η_{IPCE} peak and low J_{SC} in segments which presumably have high concentration of 4-tBP (segments 1 and 2).

3.5. Normalized IPCE spectra

In order to do a thorough analysis of the shape of the IPCE spectra and possible shifts towards blue or red, normalization is applied in order to remove any wavelength independent variations. In order to study the spectrum shift, values at the half maximum (normalized spectra at 0.5) are compared. Examples of the normalized spectra for segmented cells with electrolytes 4-tBP-LiI and NMBI-LiI are presented in Figure 6.

The critical parameter in the analysis of peak shifts is the light wavelength (λ) at the half maximum QE value of the normalized IPCE spectrum, which is shown for all the cell types in Figure 7. The optical difference in the electrolyte in the case of NMBI-LiI discussed above causes the variation in the left branches / blue side (around 450 nm) of the IPCE CE spectrum while the right branches / red side (around 600 nm) remain substantially unaffected (Figure 7). Additionally, there are some differences in the shoulder (blue side, around 450 nm) of the IPCE PE spectra of NMBI-LiI cells (Figure 6c) which are caused by the optical differences. These differences are in good qualitative correspondence with previously made optical measurements of different kinds of electrolytes.[38] Other electrolytes have even color throughout the cells which results in that the half maximum λ of the IPCE CE (Figure 7a) and the shoulder at the blue side (Figure 6) and are much more uniform compared to cells with NMBI-LiI electrolyte.

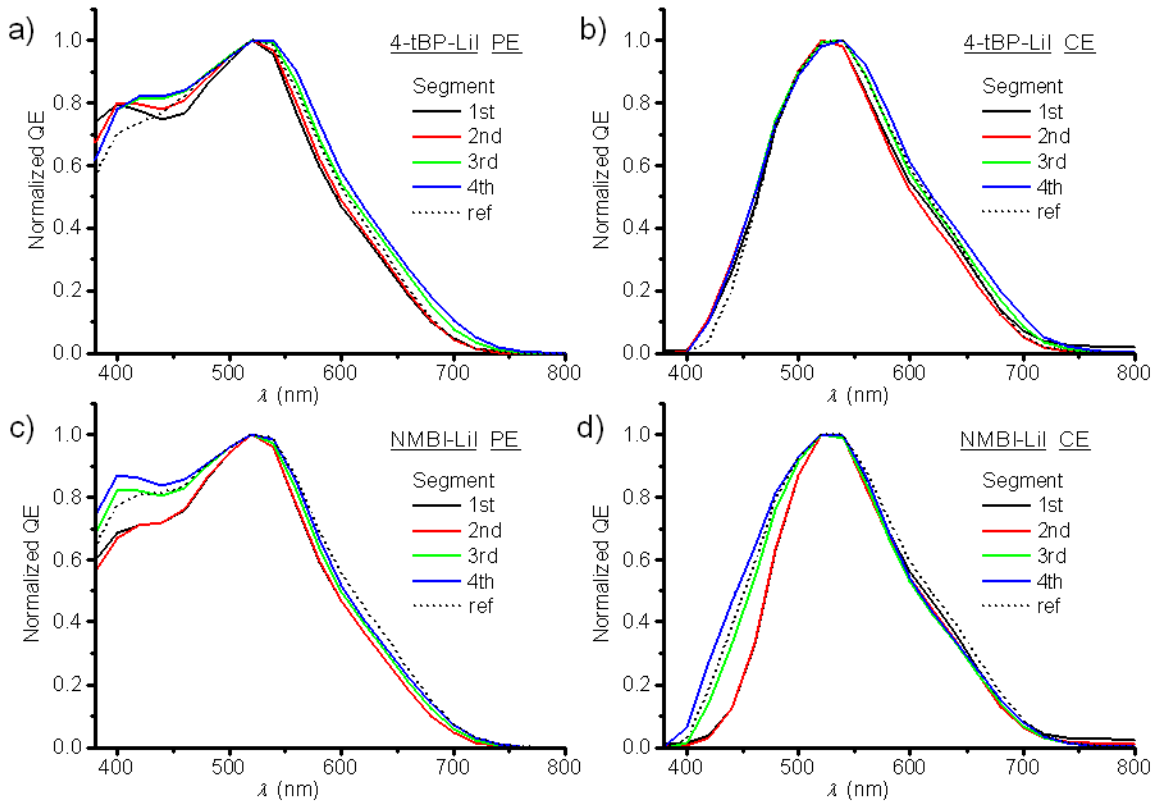

Figure 6. Normalized η_{IPCE} for segments with a,b) 4-tBP-LiI and c,d) NMBI-LiI electrolytes. a,c) PE IPCE spectra and b,d) CE IPCE spectra are respectively represented on the left and on the right side. The horizontal dashed lines show the half maximum value taken as reference for cells comparison.

Half maximum values of the normalized IPCE from CE side illumination show 20 nm IPCE blue shift (Figure 7b). It was previously mentioned that the normalized 1-T spectra showed a 15 nm shift. Hence most of the shift is related to changes in the absorption, i.e. η_{LH} of the 4-tBP-LiI cells. There may be some added effect causing the larger shift in the IPCE spectra for instance all the carboxylic acid groups present in the dye may not anchored onto the TiO_2 surface. Hence, because of the base properties of the pyridine

additives into the electrolyte in presence of 4-tBP, a dye deprotonation effect could be generated and thus changes in TiO_2 surface charge. Deprotonation is also reported to cause a blue shift in the absorption spectrum [39] and to affect negatively η_{INJ}.[32,40] Moreover, it has been reported that absorption spectra is affected by intermolecular interactions e.g. the formation of aggregates.[33,41] Katoh et al. proposed the blue shift is not caused by changes in the number of protons on the carboxylic groups of the dye because any isosbestic point does not appear in the absorbance spectra but by dye solvation which gives rise to changes in the absorption coefficient and peak position of the dye.[33] The slightly larger IPCE shift compared to normalized 1-T might be related to wavelength dependent η_{COL} or injection efficiency η_{INJ}.

Similar blue shifts in the IPCE have been shown in the literature for the addition of 4-tBP,[39] but unfortunately the effect of absorption was not quantified. The addition of Li^+ ions has been shown to shift the peak position towards longer wavelengths.[22,33,35,42,43] Considering that the data in Table 2 shows for NMBI the same effects as for 4-tBP cells, the segments with large amount of 4-tBP or NMBI (near the electrolyte filling hole, i.e. highest in segment 1) should report a blue shift while those with Li^+ (possibly farthest from the filling hole, i.e. highest in segment 4) a red shift. This behavior is seen clearly in Figures 6 and 7 where the total shift from segment 1 to segment 4 is almost 20 nm for 4-tBP and 10 nm for NMBI.

The larger shift for 4-tBP could be caused by different complex formation occurring among electrolyte additives. Intermolecular interactions such as formation of complexes between

4-tBP and Li^+ as well as NMBI and Li^+ has been verified in the literature.[22,33,44] As proposed by Katoh et al.,[33] because of this complex formation, the concentration of Li^+ ions on TiO_2 surface would decrease, while it would increase in the free electrolyte solution in the cell. This phenomenon would then increase the amount of 4-tBP adsorbed on the surface of TiO_2.[33] If this latter phenomenon occurred for NMBI additive as well, but with smaller intensity, it may explain the larger blue shift in the segmented cell with 4-tBP-LiI compared to the other cells which contain NMBI (Figure 7b).

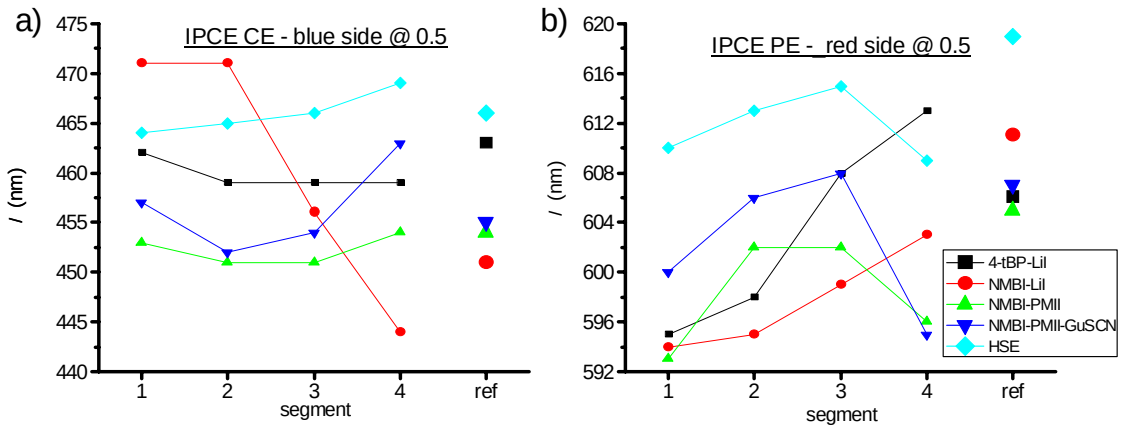

Figure 7. λ values at the half maximum of the normalized IPCE CE illumination for a) the blue side and d) λ values at half maximum of the normalized IPCE PE illumination for the red side of the spectrum. Increase in λ relates to red shifting whereas decrease in λ a blue shifting. All of these values are presented for 4-segments cells and small reference cells with the different electrolytes.

4. Conclusions

We have demonstrated that the molecular filtering effect known from chromatography has a significant impact on DSC performance. The presence of this phenomenon has not been

appreciated previously. Our results show significant spatial variations and efficiency losses up to 35 % as the cell size was increased from 0.4 cm^2 to 1.6 cm^2. These large variations are therefore in laboratory sized cells, which have typical sizes of 0.25 - 2 cm^2. More importantly, the relevance to industry is even greater since if there are large variations on a laboratory scale, there are likely to be even larger ones as device size is increased further. Uneven spatial performance could be one of the largest loss mechanisms in up-scaling DSC technology and can partly explain the difference observed between small champion cells and larger sub-modules

The apparent accumulation of 4-tBP, NMBI and effective loss Li^+ is expected to shift the conduction band of TiO_2 higher and reduce electron injection but here they may also affect dye regeneration: The Raman data showed a good correlation between the SCN^- peak intensity and J_{SC}. The SCN^- ligands have been previously been shown to play an important role in the regeneration of dye and the substitution of SCN^- ligands to be sensitive to the concentration changes of 4-tBP, NMBI and Li^+. The reduced spatial variations when replacing LiI with PMII in the electrolyte were interpreted to be related to the ability of bulky PMI^+ cations to protect SCN^- ligands better from exchange reactions compared to small Li^+.

The spatial effects are widespread as variation is seen with all the 5 different electrolyte compositions which are representative of those normally used in the field. The efficiency losses were the largest (35 %) with conventional 4-tBP-LiI electrolyte. Using a modern NMBI-PMII-GuSCN electrolyte or a commercially available high stability electrolyte, the

losses were reduced to 10 %. The efficiency losses are, however, still important from an industrial point of view. Moreover, we note that practically all the liquid electrolytes which have been shown to give good stability and performance include either tBP, NMBI or similar additives such as benzimidazole. Here the molecular filtering effect was seen to cause problems with both tBP and NMBI. Hence finding a commercially interesting electrolyte composition which would not be prone to this effect remains a challenge.

Acknowledgements

K.M. is grateful for Finnish Foundation for Technology Promotion (Tekniikan edistämissäätiö) for a post doctoral grant. This work was partly in the project Carbon NanoBud-based Energy Systems for Mobile Devices, CNB-E, of the TKK/Aalto University Multidisciplinary Institute of Digitalisation and Energy, MIDE.

Lisää viite :

Fischer, H. Pettersson, A, Hagfeldt, G. Boschloo, L. Kloo, M. Gorlov, Sol. Energy Mat. Sol. Cells 2007, 91, 1062-1065.

References

[1] M.A. Green, K. Emery, Y. Hishikawa and W. Warta, Prog. Photovolt: Res. Appl., 2011, 19, 84-92.

[2] R. Sastrawan, J. Beier, U. Belledin, S. Hemming, A. Hinsch, R. Kern, C. Vetter, F.M. Petrat, A. Prodi-Schwab, P. Lechner and W. Hoffmann, Prog. Photovolt: Res. Appl., 2006, 14, 697-709.

[3] M. Späth, P.M. Sommeling, J.A.M. van Roosmalen, H.J.P. Smit, N.P.G. van der Burg, D.R. Mahieu, N.J. Bakker and J.M. Kroon, Prog. Photovolt: Res. Appl., 2003, 11, 207-220.

[4] R. Sastrawan, J. Beier, U. Belledin, S. Hemming, A. Hinsch, R. Kern, C. Vetter, F.M. Petrat, A. Prodi-Schwab, P. Lechner and W. Hoffmann, Sol. Energy Mater. Sol. Cells, 2006, 90, 1680-1691.

[5] K. Miettunen, J. Halme and P. Lund, Electrochem. Comm., 2009, 11, 25-27.

[6] M. Toivola, T. Peltola, K. Miettunen, J. Halme and P. Lund, J. Nanosci. Nanotech., 2010, 10, 1078-1084.

[7] B. Macht, M. Turrión, A. Barkschat, P. Salvador, K. Ellmer and H. Tributsch, Sol. Energy Mater. Sol. Cells, 2004, 83, 247-262.

[8] A. Hagen, A. Barkschat, J.K. Dorhmann and H. Tributsch, Sol. Energy Mater. Sol. Cells, 2003, 77, 1-13.

[9] K. Miettunen, J. Halme, A.-M. Visuri and P. Lund, J. Phys. Chem. C, 2011, 115, 7019-7031.

[10] P.M. Sommeling, M. Späth, H.J.P. Smith, N.J. Bakker, and J.M. Kroon, J. Photochem. Photobio. A. Chem., 2004, 164, 137-144.

[11] A. Fischer, H. Pettersson, A, Hagfeldt, G. Boschloo, L. Kloo, and M. Gorlov, Sol. Energy Mat. Sol. Cells, 2007, 91, 1062-1065.

[12] K. Hara, Y. Dan-oh, C. Kasada, Y. Ohga, A. Shinpo, S. Sadaharu, K. Sayama and H. Arakawa, Langmuir, 2004, 20, 4205-4210.

[13] S. Nakade, T. Kanzaki, W. Kubo, T. Kitamura, Y. Wada, and S. Yanagida J. Phys. Chem. B, 2005, 109, 3480–3487.

[14] C. Kontoyannis, M. Orkoula and P. Koutsoukos, Analyst, 1997, 122, 33-38.

[15] C. Shi, S. Dai, K. Wang, X. Pan, F. Kong and L. Hu, Vib. Spectrosc., 2005, 39, 99-105.

[16] H. Greijer Agrell, J. Lindgren and A. Hagfeldt, J. Photochem. Photobio. A: Chem., 2004, 164, 23-27.

[17] H. Greijer, J. Lindgren and A. Hagfeldt J. Phys. Chem. B, 2001, 105, 6314–6320.

[18] F. Nour-Mohammadi, H. T. Nguyen, G. Boschloo, and T. Lund. J. Photochem. Photobio. A, 2007, 187, 348-355.

[19] Md. K. Nazeeruddin, P.Péchy, T. Renouard, S.M. Zakeeruddin, R. Humphry-Baker, P. Comte, P. Liska, L. Cevey, E. Costa, V. Shklover, L. Spiccia, G. B. Deacon, C. A. Bignozzi and M. Grätzel, J. Am. Chem. Soc., 2001, 123, 1613-1624.

[20] Md. K. Nazeeruddin, P. Péchy and M. Grätzel, Chem. Commun., 1997, 18, 1705-1706.

[21] A.R. Andersen, J. Halme, T. Lund, M.I. Asghar, P. T. Ngyuen, K. Miettunen, E. Kemppainen and O. Albrektsen. J. Phys. Chem. C, 2011, 115, 15598-15606.

[22] J. R. Jennings and Q. Wang, J. Phys. Chem. C, 2010, 114, 1715–1724.

[23] G. Schlichthörl, S.Y. Huang, J. Sprague and A.J. Frank, J. Phys. Chem. B, 1997, 101 8141-8155.

[24] K. Hara, T. Horiguchi, T. Kinoshita, K. Sayama and H. Arakawa, Solar Energy Mater. Solar Cells., 2001, 70, 151-161.

[25] C. Zhang, J. Dai, Z. Huo, X. Pan, L. Hu, F. Kong, Y. Huang, Y. Sui, X. Fang, K. Wang and S. Dai, Electrochem. Acta, 2008, 53 5503-5508.

[26] H.-L. Lu, Y.-H. Lee, S.-T. Huang, C. Su and T. Yang, Solar Energy Mater. Solar Cells, 2011, 95, 158-162.

[27] S. E. Koops, B. C. O'Regan, P. R. F. Barnes and J. R. Durrant, J. Am. Chem. Soc., 2009, 131, 4808-4818.

[28] M.K. Nazeeruddin, A. Kay, I. Rodicio, R. Humphry-Baker, E. Müller, P. Liska, N. Vlachopoulos and M. Grätzel, J. Am. Chem. Soc., 1993, 115, 6382-6390.

[29] J. Halme, G. Boschloo, A. Hagfeldt and P. Lund, J. Phys. Chem. C, 2008, 112, 5623-5637.

[30] Y. Liu, A. Hagfeldt, X.R. Xiao and S.E. Lindquist, Solar Energy Mater. Solar Cells., 1998, 55, 267-281.

[31] A. Onicha and F. Castellano, J. Phys. Chem. C, 2010, 114, 6831–6840.

[32] Y. Tachibana, Md. K. Nazeeruddin, M. Grätzel, D. Klug and J.R. Durrant, Chem. Phys., 2002, 285, 127-132.

[33] R. Katoh, M. Kasuya, S. Kodate, A. Furube, N. Fuke and N. Koide, J. Phys. Chem. C, 2009, 113, 20738-20744.

[34] A. Y. Anderson, P. R. F. Barnes, J. R. Durrant and B. C. O'Regan, J. Phys. Chem. C, 2011, 115, 2439-2447.

[35] H. Wang, J. Bell, J. Desilvestro, M. Bertoz and G. Evans, J. Phys. Chem. C, 2007, 111, 15125–15131.

[36] S. Pelet, J.-E. Moser and M. Grätzel, J. Phys. Chem. B, 2000, 104, 1791-1795.

[37] S. Nakade, T. Kanzaki, W. Kubo, T. Kitamura, Y. Wada and S. Yanagida J. Phys. Chem. B, 2005, 109, 3480–3487.

[38] K. Miettunen, M.Sc. Thesis, 2006, Helsinki University of Technology.

[39] G. Boschloo, H. Lindström, E. Magnusson, A. Holmberg and A. Hagfeldt, J. Photochem. Photobio. A: Chem., 2002, 148, 11-15.

[40] S.A. Hague, E. Palomares, B.M. Cho, N.M. Green, N. Hirata, D.R. Klug and J.R. Durrant, J. Am. Chem. Soc., 2005, 127, 3456-3462.

[41] A. Furube, M. Murai, Y. Tamaki, S. Watanabe and R. Katoh, J. Phys. Chem. A, 2006, 110, 6465.

[42] C. Kelly, F. Farzad, D. Thompson, J. Stipkala and G. Meyer, Langmuir, 1999, 15, 7047–7054.

[43] A. Staniszewski, S. Ardo, Y. Sun, F. Castellano and G. Meyer, J. Am. Chem. Soc., 2008, 130, 11586-11587.

[44] M. Grätzel, Inorg. Chem., 2005, 44, 6841-6851.